

On the evolutionary trail of MagRs

Jing Zhang^{1,2}, Yafei Chang^{1,2}, Peng Zhang^{1,2}, Yanqi Zhang^{1,2}, Mengke Wei³, Chenyang Han³, Shun Wang³, Hui-Meng Lu⁴, Tiantian Cai^{1,2,5,*}, Can Xie^{1,2,5,*}

¹ High Magnetic Field Laboratory, Hefei Institutes of Physical Science, Chinese Academy of Sciences, Science Island, Hefei, Anhui 230031, China

² Science Island Branch of Graduate School, University of Science and Technology of China, Hefei, Anhui 230036, China

³ Institutes of Physical Science and Information Technology, Anhui University, Hefei, Anhui 230039, China

⁴ School of Life Sciences, Key Laboratory for Space Bioscience and Biotechnology, Northwestern Polytechnical University, Xi'an, Shaanxi 710072, China

⁵ Institute of Quantum Sensing, Zhejiang University, Hangzhou, Zhejiang 310027, China

ABSTRACT

Magnetic sense, or termed magnetoreception, has evolved in a broad range of taxa within the animal kingdom to facilitate orientation and navigation. MagRs, highly conserved A-type iron-sulfur proteins, are widely distributed across all phyla and play essential roles in both magnetoreception and iron-sulfur cluster biogenesis. However, the evolutionary origins and functional diversification of MagRs from their prokaryotic ancestor remain unclear. In this study, MagR sequences from 131 species, ranging from bacteria to humans, were selected for analysis, with 23 representative sequences covering species from prokaryotes to Mollusca, Arthropoda, Osteichthyes, Reptilia, Aves, and mammals chosen for protein expression and purification. Biochemical studies revealed a gradual increase in total iron content in MagRs during evolution. Three types of MagRs were identified, each with distinct iron and/or iron-sulfur cluster binding capacity and protein stability, indicating continuous expansion of the functional roles of MagRs during speciation and evolution. This evolutionary biochemical study provides valuable insights into how evolution shapes the physical and chemical properties of biological molecules such as MagRs and how these properties influence the evolutionary trajectories of MagRs.

Keywords: Magnetoreception; Magnetoreceptor (MagR); Iron-sulfur cluster; Stability; Evolutionary biochemistry

INTRODUCTION

The Earth's geomagnetic field is a natural environmental

This is an open-access article distributed under the terms of the Creative Commons Attribution Non-Commercial License (<http://creativecommons.org/licenses/by-nc/4.0/>), which permits unrestricted non-commercial use, distribution, and reproduction in any medium, provided the original work is properly cited.

Copyright ©2024 Editorial Office of Zoological Research, Kunming Institute of Zoology, Chinese Academy of Sciences

component influencing all living organisms during evolution. Magnetic sense, or magnetoreception, has evolved across a broad range of animal taxa to facilitate orientation and navigation (Begall et al., 2013; Johnsen & Lohmann, 2008; Mouritsen, 2018; Qin et al., 2016; Wang et al., 2023; Wiltschko & Wiltschko, 1995, 2006, 2005). This sensory ability enables the extraction of two types of information: (1) directional or “compass” information, and (2) positional or “map” information. These are derived from three geomagnetic field parameters, including polarity (direction of the horizontal component), inclination (angle between the Earth's magnetic field lines and its surface), and intensity (Naisbett-Jones & Lohmann, 2022).

Several models have been proposed to explain the mechanism underlying animal magnetoreception, including the magnetite-based model for polarity detection (Cadiou & McNaughton, 2010; Kirschvink & Gould, 1981; Kirschvink et al., 2001; Walcott et al., 1979), the cryptochrome (Cry)-based radical-pair model or quantum compass for inclination detection (Hore & Mouritsen, 2016; Maeda et al., 2008; Ritz et al., 2000; Rodgers & Hore, 2009; Schulten & Weller, 1978), and the MagR/Cry-based biocompass model for both polarity and inclination detection (Lohmann, 2016; Qin et al., 2016; Xie, 2022).

Remarkably diverse animals, from invertebrates such as mollusks and insects to vertebrates such as sea turtles and birds, perceive guidance cues from the geomagnetic field. Different organisms inhabit various environments, ranging from oceans to land and air, and may have undergone distinct evolutionary paths to sense and utilize geomagnetic field cues for various purposes including long-distance migration, short-distance movement, homing, nesting, body alignment, and food searching. In the ocean, the marine mollusk *Tritonia*

Received: 05 March 2024; Accepted: 22 April 2024; Online: 23 April 2024

Foundation items: This study was supported by the National Natural Science Foundation of China (31640001 and T2350005 to C.X.), Ministry of Science and Technology of China (2021ZD0140300 to C.X.), and Presidential Foundation of Hefei Institutes of Physical Science, Chinese Academy of Sciences (Y96XC11131, E26CCG27, and E26CCD15 to C.X., E36CWGBR24B and E36CZG14132 to T.C.)

*Corresponding authors, E-mail: tiantiancai@zju.edu.cn; canxie@zju.edu.cn

diomedea can orient to the Earth's magnetic field to navigate between shallow and deeper areas (Lohmann & Willows, 1987). Salmon, coral reef fish, lobsters, and sea turtles also exhibit magnetic sense for navigation (Naisbett-Jones & Lohmann, 2022). On land, termites (*Amitermes meridionalis*) use geomagnetic cues for mound construction (Jacklyn & Munro, 2002), while mole-rats display a strong innate preference for building nests in the southeastern sector of circular arenas (Burda et al., 2020, 1990) and can navigate over both short and long distances (Kimchi et al., 2004). In the air, monarch butterflies (*Danaus plexippus*) take four generations to complete a migration of approximately 8 000 km from Mexico, across the USA to Canada, and back annually (Brower, 1996). Birds, the most mobile creatures in the animal kingdom, often undertake long-distance annual journeys guided by their innate magnetic sense (Wiltschko & Wiltschko, 2019). The Arctic tern (*Sterna paradisaea*) completes the longest roundtrip migration annually, traveling from pole to pole (Alerstam et al., 2019; Egevang et al., 2010). Both the migratory European robin (*Erithacus rubecula*) and homing pigeon (*Columba livia*) have been extensively studied in the field and laboratory for their ability to sense the geomagnetic field during navigation (Biro, 2010; Mouritsen & Ritz, 2005; Qin et al., 2016; Wang et al., 2024; Wiltschko & Wiltschko, 2006; Xie, 2022; Xu et al., 2021; Zhou et al., 2023). Of note, the existence of a human magnetic sense remains the subject of ongoing study, debate, and controversy (Baker, 1980, 1988; Chae et al., 2022; Foley et al., 2011; Wang et al., 2019; Westby & Partridge, 1986).

The broad distribution and phylogenetic diversity of animals with a magnetic sense suggest that this sensory modality evolved before the major evolutionary radiations, motivating the exploration of the evolutionary history of the putative magnetoreceptor. In the biocompass model, the magnetoreceptor MagR forms a rod-like complex with Cry, indicating a possible mechanism of biomagnetism and implying a connection between the biocompass and quantum compass (Xie, 2022).

MagRs, or the homologous bacterial iron-sulfur cluster assembly (IscA) protein, are dual-functional proteins involved in both magnetoreception and iron-sulfur cluster (Fe-S) biogenesis and are highly evolutionarily conserved from bacteria to humans (Lu et al., 2020). MagRs exhibit various unique and sophisticated features. First, the binding of iron and/or iron-sulfur clusters in MagRs is highly complex and likely species-specific. In *Escherichia coli*, IscA (eIscA), the homologous protein of eukaryotic MagRs, binds to iron (Ding & Clark, 2004; Ding et al., 2007; Landry et al., 2013), while in pigeons and humans, MagRs bind to both iron and iron-sulfur clusters (Guo et al., 2021; Song et al., 2009; Weiler et al., 2020; Zhou et al., 2023). Additionally, two forms of iron-sulfur clusters [2Fe-2S] and [3Fe-4S] have been identified in pigeon MagR, which show different magnetic properties (Guo et al., 2021), potentially serving as a magnetic switch to modulate magnetoreceptor sensitivity. Second, the functional roles of the N-terminal sequences in MagRs remain incompletely understood. The highly variable N-terminal region of MagRs, present only in eukaryotic MagR/IscA1 and not in prokaryotic IscA, is proposed to play essential roles in the formation of MagR tetramers and the MagR/Cry biocompass complex, as evidenced by sequence analysis and molecular dynamics (Friis et al., 2017; Lu et al., 2020) and recently validated by biochemical analysis in pigeon MagR (Zhang et al., 2024).

The same region also contributes to the high affinity binding of iron and iron-sulfur clusters (Zhang et al., 2024). Furthermore, the MagR proteins from European robin and pigeon differ markedly in their iron and iron-sulfur binding capacity and conformation, despite only three residues varying between them (Wang et al., 2024). Therefore, elucidating the conservation and variation of this dual-functional protein from both sequence and biochemical perspectives will extend our understanding of MagRs as iron-sulfur cluster proteins and magnetoreceptors.

In this study, MagR sequences from 131 species across a wide range of taxa, from bacteria to humans, were analyzed, with 23 representative sequences selected for protein expression and purification. The biochemical properties of the 23 MagR proteins from different species were compared, leading to the identification of three distinct types based on their iron and iron-sulfur cluster binding capacities. Interestingly, the binding capacity for iron and iron-sulfur clusters in MagR proteins increased progressively from prokaryotes to mammals, correlating with the increasing body complexity. Furthermore, iron-sulfur cluster binding appears to be a requisite feature of eukaryotic MagRs, in addition to the mononuclear iron binding observed in bacterial IscA. Four MagRs from bacteria, worms, and pigeons and humans, representing the three different types, were selected for further systematic analysis and comparison. The stability of MagRs was also found to increase gradually during evolution and speciation. Overall, this study provides a comprehensive overview of the evolutionary trajectory of MagRs, both as iron-sulfur proteins and magnetoreceptors, shedding light on how animal magnetoreception evolved from an ancient prokaryotic iron-sulfur protein.

MATERIALS AND METHODS

Multiple sequence alignment and phylogenetic analysis

The MagR and IscA protein sequences from 131 species were downloaded from the NCBI database. The common English name of the species and accession numbers of the protein sequences are provided in Supplementary Figure S1 alongside each sequence. The MagR sequences from the monarch butterfly and pigeon were obtained from a previous study (Qin et al., 2016), while the MagR sequence from the sea slug (*Elysia leucolegnote*) was shared by Dr. Yinglang Wan from Hainan University. All sequences were aligned using ClustalW (<https://www.megasoftware.net/citations>) and colored according to identity percentage with ESPript v.3.0 (<https://esript.ibcp.fr/ESPript/ESPript/index.php>) (Figure 1A; Supplementary Figure S1). Among these sequences, 23 representatives were chosen for further phylogenetic analysis and protein expression and purification. A phylogenetic tree of these 23 MagRs from different species was also constructed using MEGA v.7.0. Evolutionary history was inferred using the neighbor-joining method and the Poisson model (Saitou & Nei, 1987). Rates among sites were calculated using the uniform rate and gaps/missing data were treated by complete deletion. The bootstrap consensus tree inferred from 1 000 replicates was taken to represent the evolutionary history of the taxa analyzed (Felsenstein, 1985). The percentage of replicate trees in which the associated taxa clustered together in the bootstrap test (1 000 replicates) is shown next to the branches (Felsenstein, 1985). The evolutionary distances were computed using the Poisson correction method (Kaur et al., 2018), expressed as the number of amino acid substitutions

per site.

Protein expression and purification

The DNA sequences encoding the 23 representative MagR proteins were codon-optimized and synthesized for *E. coli* expression (Songon Biotech, China). The expression vectors containing *MagR* gene sequences were constructed as described previously (Qin et al., 2016). All MagR proteins were expressed in *E. coli* strain BL21 (DE3) with a Strep-II tag fused to the N-terminal. After induction with 20 $\mu\text{mol/L}$ isopropyl-D-1-thiogalactopyranoside (IPTG) at 15°C for 20 h, cells were harvested, resuspended in lysis buffer (20 mmol/L Tris, 500 mmol/L NaCl, pH 8.0), and lysed by sonication on ice. Following centrifugation at 17 500 r/min for 45 min at 4°C, the supernatants were collected and loaded onto Strep-Tactin affinity columns (IBA GmbH, Germany). The resin was washed with 50 resin volumes of washing buffer (20 mmol/L Tris, 500 mmol/L NaCl, pH 8.0) to remove unbound proteins. The target proteins were then eluted with elution buffer (20 mmol/L Tris, 500 mmol/L NaCl, 5 mmol/L desthiobiotin, pH 8.0). The purity of all purified proteins was verified with sodium dodecyl-sulfate polyacrylamide gel electrophoresis (SDS-PAGE), with PageRuler Prestained Protein Ladder (Thermo Fisher Scientific, USA) used as the molecular weight standard. Protein concentration was estimated by measuring absorption at 280 nm with a NanoDrop spectrophotometer (NanoDrop OneC, Thermo Scientific, USA).

Electron paramagnetic resonance measurement

X-band (9.6 GHz) electron paramagnetic resonance (EPR) spectra were recorded using an EMX plus 10/12 spectrometer (Bruker, Billerica, MA) equipped with an Oxford ESR-910 liquid helium cryostat. For oxidized protein samples, 50 μL of glycerol was added to 200 μL of 1 mmol/L sample. The protein samples were then injected into quartz EPR tubes (Wilmad 707-SQ-250 M, USA) and frozen with liquid nitrogen. The EPR signals were collected at different temperatures (10 K, 25 K, 45 K, and 60 K) under a microwave frequency of 9.40 GHz, microwave power of 2 mW, modulation amplitude of 2.0 G, and receive gain of 1.0×10^4 .

Ultraviolet-visible (UV-Vis) absorption analysis and circular dichroism (CD) spectroscopy

The UV-Vis absorption spectra of MagR proteins were measured from 300 nm to 600 nm using a NanoDrop spectrophotometer (Thermo Scientific, NanoDrop OneC, USA) at room temperature. For the regular characterization of iron and iron-sulfur cluster binding, 100 $\mu\text{mol/L}$ MagR proteins were used (Figures 2, 3, 4A). To compare the stability of MagR proteins, UV-Vis spectra with time-lapse experiments were collected with 200 $\mu\text{mol/L}$ MagR proteins (Figure 5). Color variation of the MagR proteins from different species was compared in solution at a concentration of 500 $\mu\text{mol/L}$ (Figure 4A).

The protein-bound metals and iron-sulfur clusters in the MagR proteins were measured using a CD spectrometer MOS-500 (Biologic, France) at room temperature. The purified proteins (10 $\mu\text{mol/L}$) were prepared in 20 mmol/L phosphate buffer (pH 8.0).

Ferrozine assay

A stable purplish-red compound was formed by the interaction of ferrous iron with ferrozine, showing a characteristic absorption peak at 562 nm (Im et al., 2013). Total iron content of the proteins was determined by quantitatively reducing Fe^{3+}

to Fe^{2+} using hydroxylamine-HCl (10% (w/v) HAHCl in 1 mol/L HCl) and measuring absorption at 562 nm. The standard curve used for quantification was generated using a series of ferric chloride (FeCl_3) concentrations (0.1–1.0 mmol/L) dissolved in 1 mol/L HCl (Supplementary Figure S2). The protein samples were prepared as described previously (Zhou et al., 2023). In brief, 80 μL of hydroxylamine-HCl (10% w/v HAHCl in 1 mol/L HCl) and 20 μL of the MagR proteins (100 $\mu\text{mol/L}$) were added to a 96-well plate (Corning, USA), then mixed well and incubated at 37°C for 30 min in the dark. Then, 100 μL of ferrozine (1 g/L ferrozine in 50% w/v ammonium acetate) was added to each well. The mixtures were incubated at 37°C for an additional 5 min in the dark. Finally, the absorption of the iron-ferrozine complex in each well was measured at 562 nm using a microplate reader (Tecan Spark, Austria). Iron content in the MagR proteins was determined using linear regression analysis in comparison with standard curves. Each protein sample was tested in three independent replicates. Histograms and statistical analysis were performed using GraphPad Prism v.9.5. Two-tailed Student's *t*-test was used to test for differences in total iron between protein samples. Statistical significance is indicated in the corresponding figures with ****: $P < 0.0001$.

Size - exclusion chromatography (SEC)

The conformational states of the 23 different MagRs were monitored and differentiated using analytical SEC. Purified proteins were injected into a Superdex 6 Increase 10/300 GL column (GE Healthcare, USA) connected to a GE AKTA FPLC purification system, operated at a flow rate of 0.5 mL/min. TBS buffer (20 mmol/L Tris, 150 mmol/L NaCl, pH 8.0) was used throughout the analysis (Supplementary Figure S3).

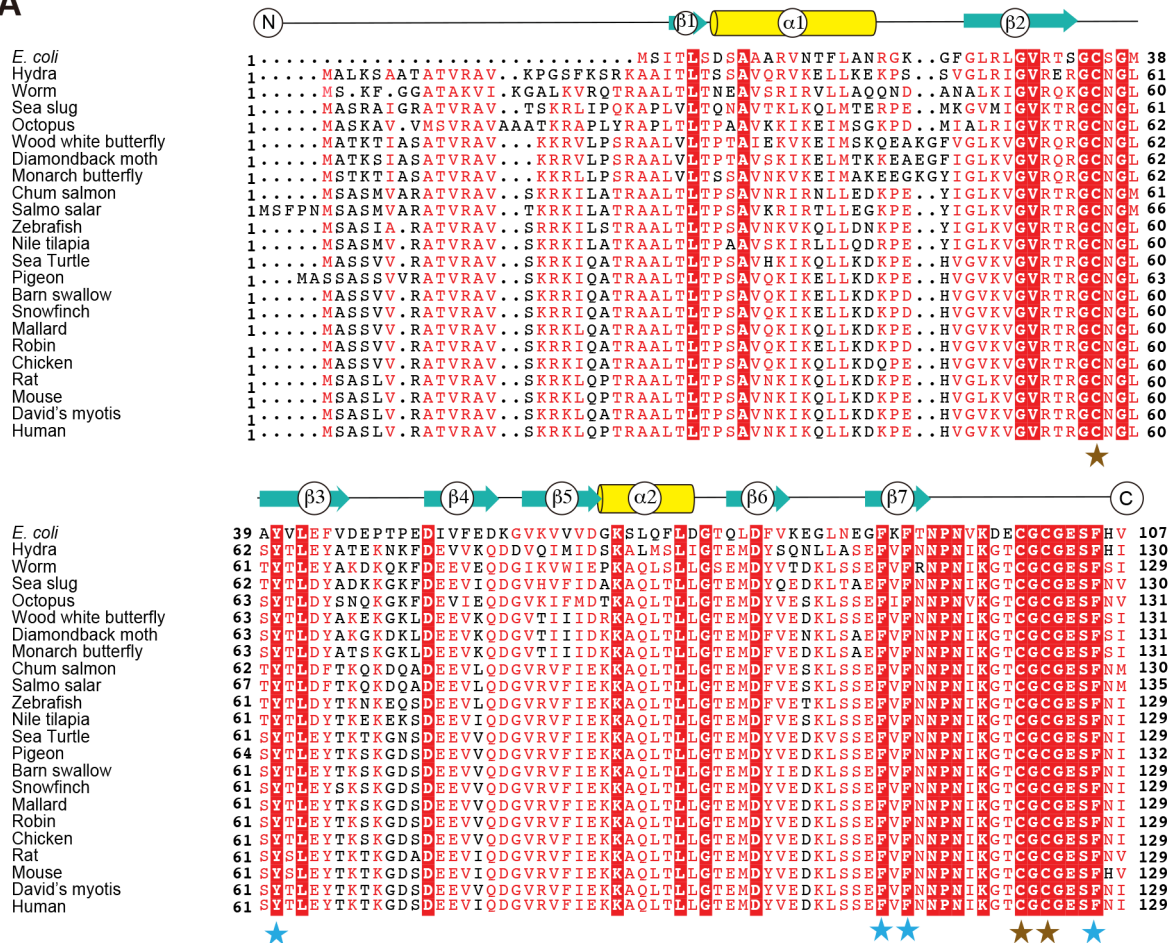
RESULTS

MagRs are highly conserved from bacteria to humans

MagR sequences from 131 species across all major phyla were retrieved from NCBI, with some re-sequenced and confirmed in previous lab work (Qin et al., 2016). Sequence alignment of all 131 MagRs (Supplementary Figure S1) and 23 representative MagRs (Figure 1A) demonstrated high MagR conservation from bacteria to humans. A notable difference between prokaryotic IscA and eukaryotic MagR/IscA is the presence of an additional 20–30 amino acids at the N-terminal of eukaryotic MagRs. The functional roles of this N-terminal sequence, such as N25 in pigeon MagR, have been extensively studied. The sequence serves not only as a mitochondrial targeting signal but also affects iron and iron-sulfur cluster binding in MagRs and the formation of the MagR/Cry complex (Zhang et al., 2024). While the C-terminal half of MagRs is highly conserved, the N-terminal half is more variable. Three cysteine residues, which form the iron-sulfur cluster binding site (Guo et al., 2021), were 100% conserved across all species (brown stars, Supplementary Figure S1; Figure 1A). Additionally, four aromatic residues, including tyrosine and phenylalanine, were also 100% conserved (blue stars, Supplementary Figure S1; Figure 1A), which may contribute to the intermolecular electron transport chain within tetramer MagRs and between MagRs and Cry (Xie, 2022).

To explore the evolutionary trajectory of MagRs in terms of biochemical properties and functions, 23 MagRs from different species (Figure 1A), spanning from prokaryotes to Mollusca, Arthropoda, Osteichthyes, Reptilia, Aves, and mammals, were carefully selected for protein expression and purification

A



B

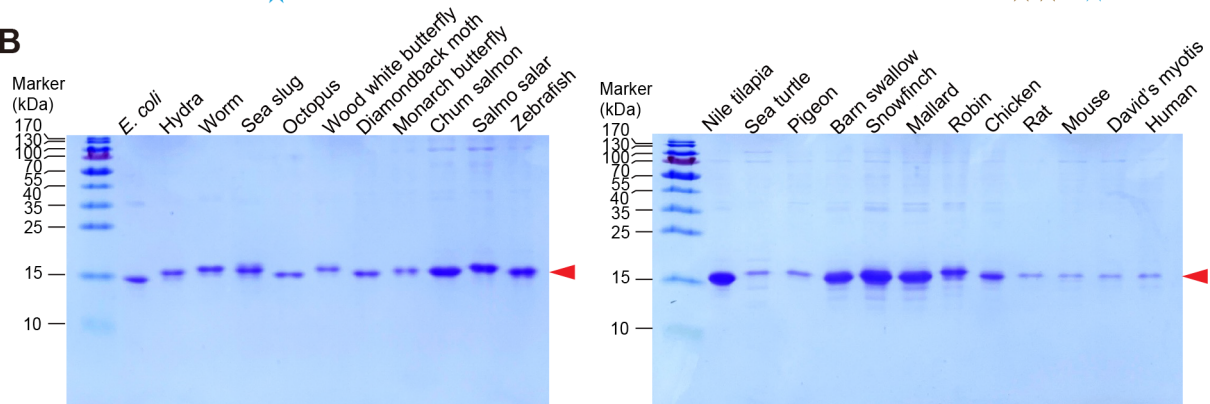


Figure 1 Sequence alignment and purification of MagRs across species

A: Sequence alignment of MagRs in 23 representative species. Residues with high similarity across species are shown in red. 100% conserved residues are shown in white with red background. Secondary structures are shown in upper lines, with two α -helices indicated by yellow cylinders and seven β -strands indicated by green arrows. Residues with iron-sulfur cluster binding properties are indicated by brown stars. Conserved residues with electron transfer properties are indicated by blue stars. B: SDS-PAGE of purified MagR proteins from 23 representative species.

(Figure 1B). All proteins were purified to homogeneity under aerobic conditions and appeared as single bands around 14–15 kDa in reduced SDS-PAGE.

Iron and iron-sulfur cluster binding capacity increases during MagR evolution

Phylogenetic trees were constructed to elucidate the evolutionary relationships of MagR proteins across species (Figure 2A). Results showed that MagRs from species within the same phylum or class clustered together in the same clade, demonstrating higher sequence similarity and closer evolutionary relationships. For example, various butterfly

species showed greater similarity to each other than to species from other classes. Comparable clustering patterns were observed for fish, birds, and mammals, likely due to both speciation and adaptation. Species within the same family share a more recent common ancestor than species from different families. Additionally, species within the same class or phylum often adapt to similar habitats, which may involve similar levels of iron metabolism.

A total of 23 MagR/IscA proteins from these species were purified to homogeneity. The purified proteins displayed various shades of brown, except for the purified bacterial IscA

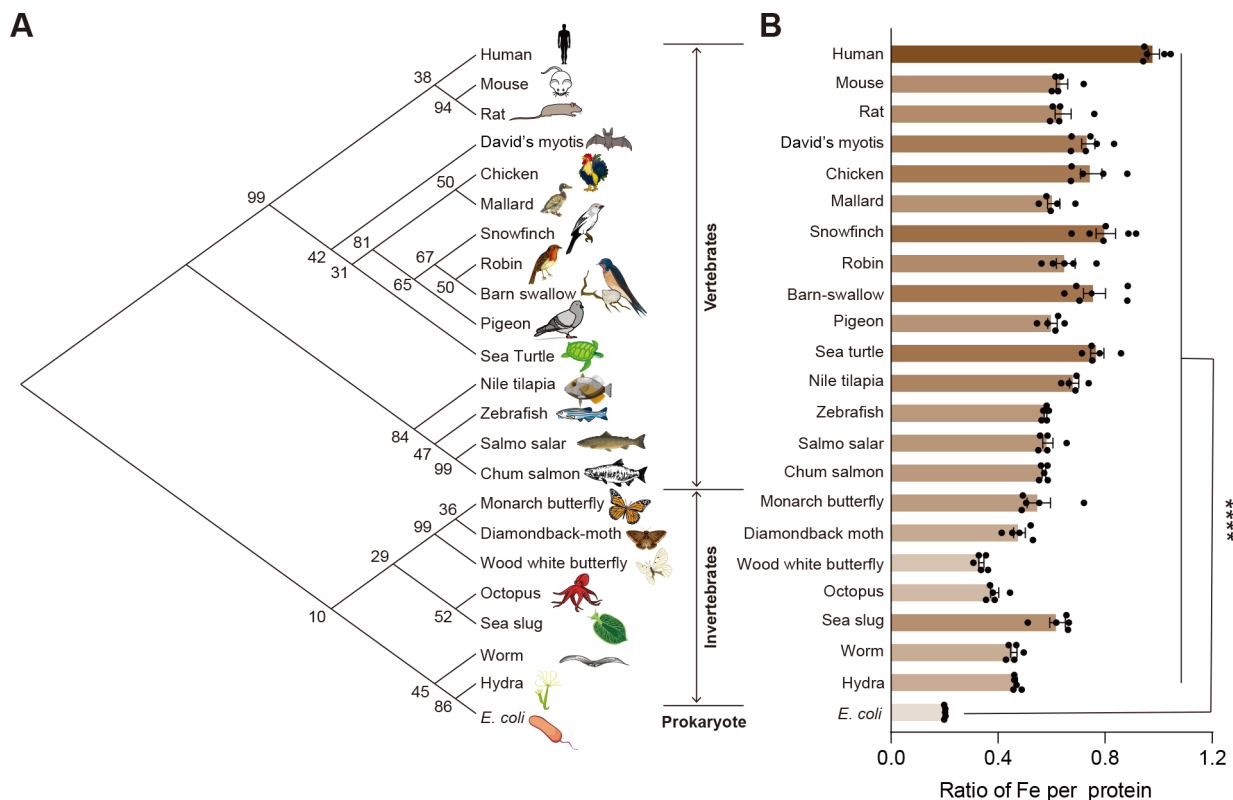


Figure 2 Molecular phylogenetic analysis and iron binding of MagR proteins

A: Phylogenetic trees of MagR protein sequences from 23 different species. Bootstrap values were obtained from 1 000 replicates using the neighbor-joining method in MEGA7 and are shown next to the branches. B: Total iron content in purified MagR proteins of 23 representative species measured by ferrozine assay as the ratio of iron atoms per protein monomer. Student's *t*-test, ****: $P < 0.0001$.

protein, which was nearly colorless. The color of the purified MagR proteins suggests possible binding of cofactors, such as iron and/or iron-sulfur clusters, consistent with previous reports of MagRs purified from different species (Cupp-Vickery et al., 2004; Ding & Clark, 2004; Ding et al., 2007; Guo et al., 2021; Landry et al., 2013; Lu et al., 2010; Nasta et al., 2019; Ollagnier-De-Choudens et al., 2001; Wang et al., 2024; Zhou et al., 2023). Cofactor binding is essential for protein function and stability. To demonstrate the iron and iron-sulfur binding capacity of MagRs during evolution, the total iron content of each MagR was measured using the ferrozine assay and compared (Figure 2B). As expected, bacterial *IscA*, the ancestral protein of eukaryotic MagRs, exhibited the lowest iron content. Generally, the MagR iron content gradually increased along the evolutionary trajectory from bacteria to humans, with some exceptions. For instance, among the invertebrates tested, the sea slug (*Elysia leucolegnote*) had the highest total iron content. Among vertebrates, the sea turtle (*Dermochelys coriacea*) and white-rumped snowfinch (*Onychostruthus taczanowskii*) exhibited high iron content in MagRs compared to other fish, amphibians, reptiles, and birds tested. Conversely, MagRs from mice (*Mus musculus*) and rats (*Rattus norvegicus*) showed relatively low total iron binding. These exceptions imply potentially unique magnetoreception abilities, which warrant further investigation.

Evolutionary biochemistry reveals evolution of three types of MagR

MagRs can bind to both mononuclear iron and iron-sulfur clusters. As total iron content measurements cannot distinguish between these two types of binding, UV-Vis spectra, CD spectra, and EPR spectra were used to further

characterize the biochemical properties of MagRs from different species.

The UV-Vis spectra of 23 purified MagR proteins from various species were measured and compared (Figure 3). In general, the UV-Vis absorption of MagRs gradually increased from bacteria to humans (Figure 3A), consistent with the color and total iron content of the purified proteins. Typically, characteristic peaks in the UV-Vis spectra at 330 nm indicate iron binding, while peaks at 330 nm, 420 nm, and 460 nm indicate iron-sulfur cluster binding of various proteins (Ding & Clark, 2004; Ding et al., 2007; Guo et al., 2021; Landry et al., 2013; Lu et al., 2010; Zhou et al., 2023).

To compare the iron-sulfur cluster binding capacity with the iron binding capacity in MagRs, the ratios of UV-Vis absorption at 420 nm or 460 nm relative to 330 nm were calculated for each MagR (Figure 3B, C). Based on the UV-Vis profiles (Figure 3A) and OD420/OD330 (Figure 3B) and OD460/OD330 (Figure 3C) absorption ratios, the 23 MagRs were classified into three different types. The first type, represented by bacterial *IscA* (*E. coli*, *eIscA*), exhibited a single prominent peak at 330 nm (Figure 3A, D), indicating it primarily binds to iron, consistent with previous reports (Ding & Clark, 2004). The second type, including MagRs from hydras (*Hydra vulgaris*), worms (*Caenorhabditis elegans*), and sea slugs (*Elysia leucolegnote*), represented by *Caenorhabditis elegans* MagR (*ceMagR*), exhibited apparent peaks at 330 nm and 420 nm, with a shoulder at 460 nm (Figure 3A, E), indicating the presence of iron-sulfur cluster binding. The third type, comprising the remaining 19 MagRs, represented by *Columba livia* MagR (*clMagR*), showed prominent peaks at 420 nm and 460 nm (Figure 3A, F), indicating significantly enhanced iron-sulfur cluster binding. These results suggest

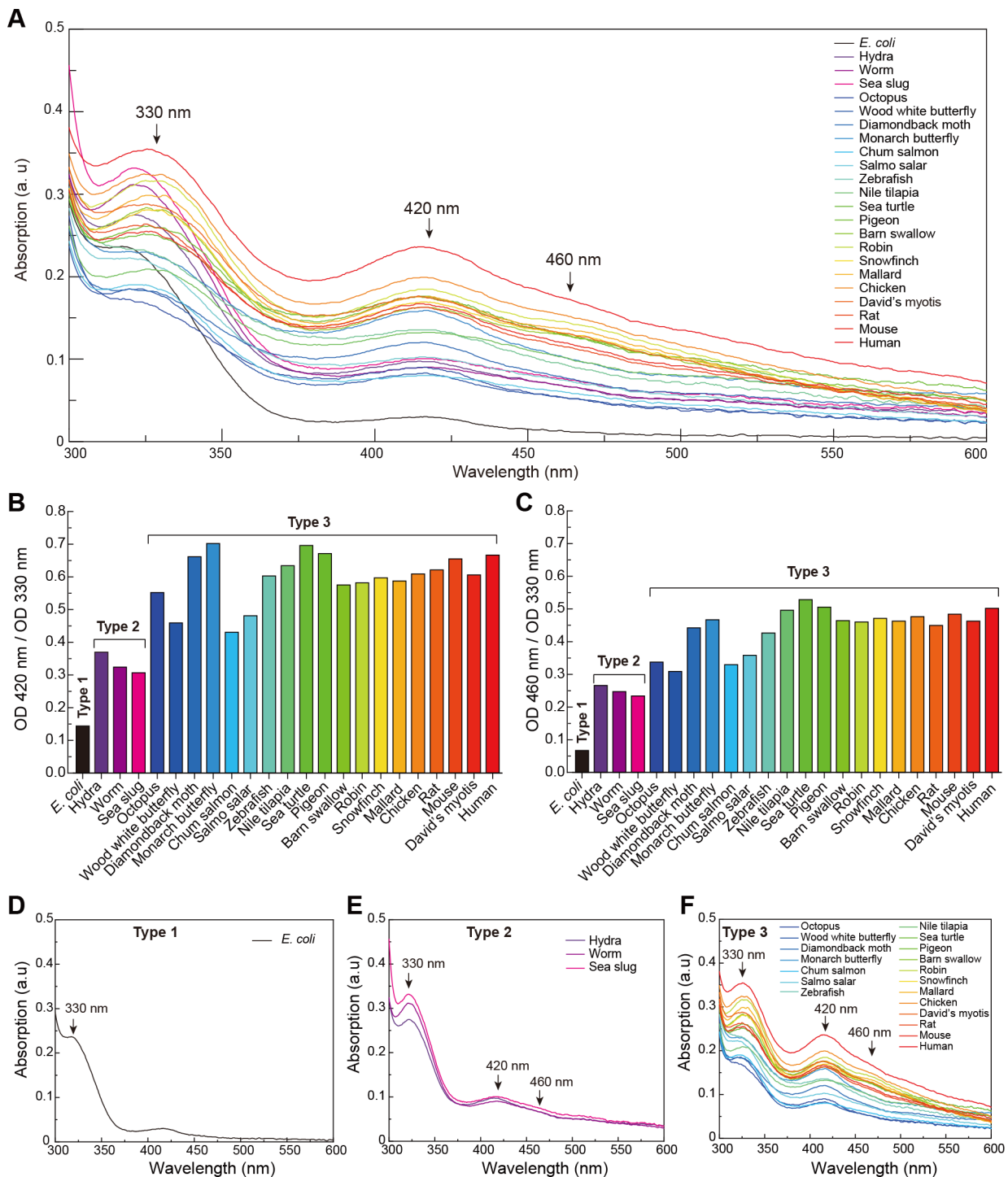


Figure 3 MagRs from different species can be classified into three different types based on UV-Vis spectra

A: UV-Vis absorption spectra of MagR proteins from 23 representative species. Typical peaks at 330 nm, 420 nm, and 460 nm are indicated with arrows. B, C: Comparison of iron-sulfur cluster binding in MagRs from 23 species was quantified by the ratio of absorption peaks at 420 nm (B) and 460 nm (C) relative to absorption peaks at 330 nm. Three types of MagRs were classified based on the ratio. D-F: UV-Vis spectra of 23 MagRs classified into three types. Type 1 MagR was represented by *eclscA* (D), type 2 MagRs were represented by three MagRs (E), and type 3 MagRs were represented by the remaining 19 MagRs.

that over the course of evolution, the extent of iron-sulfur cluster binding in MagRs has significantly increased, evolving from no binding to partial binding, and eventually to extensive binding across different species.

Late acquisition of iron-sulfur cluster binding in MagR evolution

MagRs from bacteria (*eclscA*), worms (*ceMagR*) and pigeons

and humans (*clMagR* and *hsMagR*), representing the three different types, were selected to systematically characterize and compare their biochemical features during evolution. The color of these three purified proteins varied progressively from colorless to dark brown at the same concentration (Figure 4A). Type 1 bacterial *eclscA* was colorless, while the worm *ceMagR* was light brown and the pigeon *clMagR* and human *hsMagR* were dark brown. Type 2 *ceMagR* displayed a very

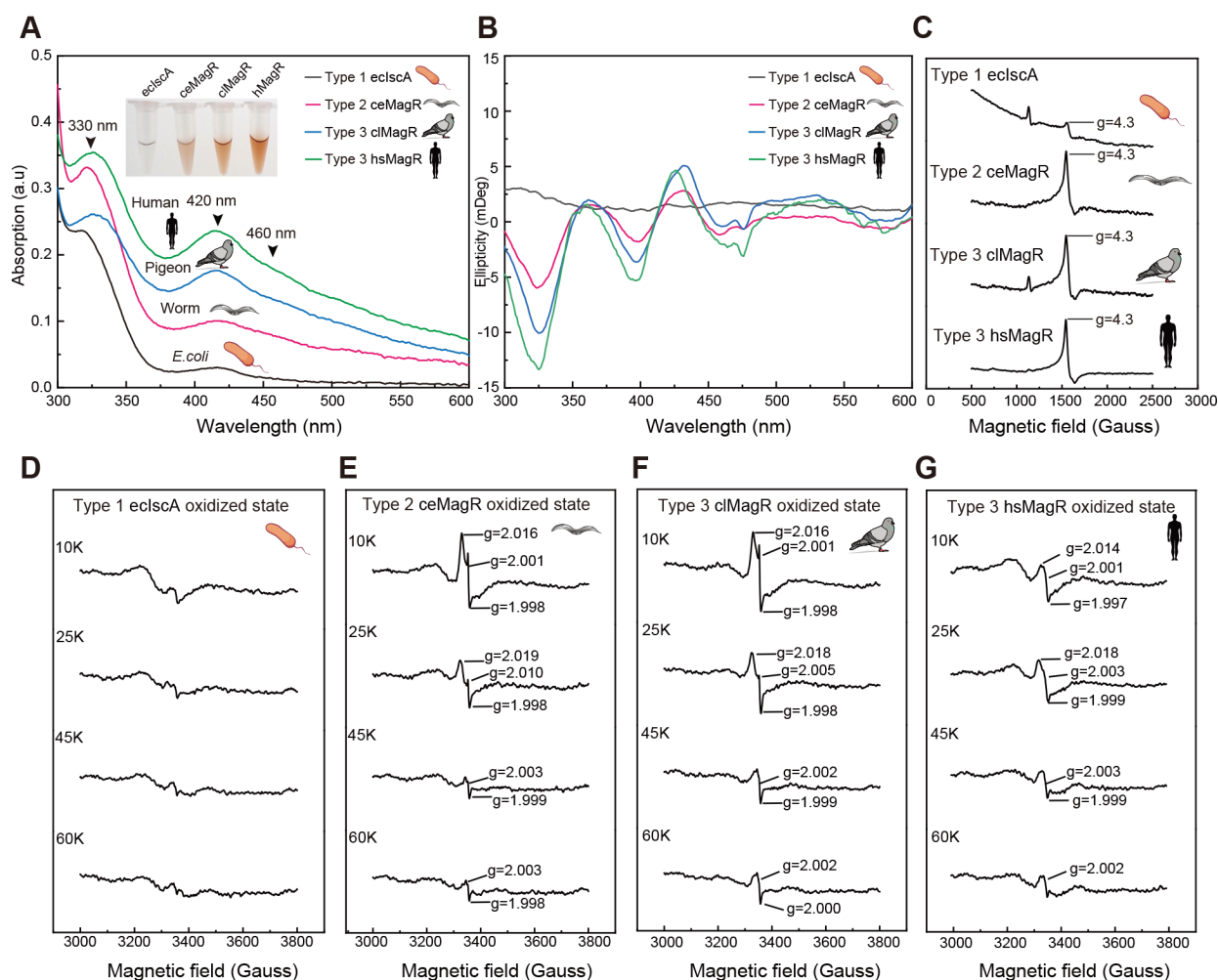


Figure 4 Iron content and types of iron-sulfur clusters in three types of MagRs

A: UV-Vis absorption spectra of purified MagR or IscA type proteins. Insert picture shows protein solution. B: CD spectra of purified eclscA (black line), ceMagR (red line), and clMagR (blue line) and hsMagR (green line), representing the three types of MagR proteins, respectively. C: Comparison of EPR spectra recorded at 10 K for eclscA, ceMagR, clMagR, and hsMagR to detect ferric iron binding in three types of MagR proteins. D–G: EPR spectra of eclscA (D), ceMagR (E), and clMagR (F) and hsMagR (G) representing three types of MagR proteins, respectively.

high absorption peak at 330 nm, while type 3 clMagR and hsMagR exhibited significant absorption peaks at 420 nm and 460 nm, indicating stronger iron-sulfur cluster binding. These findings are consistent with the UV-Vis profiles (Figure 4A) and iron content results (Figure 2B), indicating increased binding to iron-sulfur clusters in type 3 MagRs.

CD spectroscopy was employed to characterize the types of iron-sulfur clusters and their protein environments during cluster maturation. Of note, ceMagR, clMagR, and hsMagR, but not eclscA, showed distinct positive peaks at 371 nm and 426 nm and three negative peaks at 324 nm, 396 nm, and 463 nm, indicating the presence of [2Fe-2S] in the worm ceMagR, pigeon clMagR, and human hsMagR, but not in bacterial eclscA (Figure 4B). To further characterize the type of iron-sulfur clusters in MagRs, EPR spectroscopy was applied as the CD spectra alone could not exclude the possible presence of [4Fe-4S] and [3Fe-4S]. The oxidized [3Fe-4S] cluster is characterized by a rhombic EPR signal with g values at $g_1=2.016$, $g_2=2.002$, and $g_3=1.96$, disappearing at 45 K (Hoppe et al., 2011; Pandelia et al., 2011; Rothery et al., 2001). Consequently, two distinct iron-sulfur clusters, [2Fe-2S] and [3Fe-4S], were detected in the worm ceMagR, pigeon clMagR, and human hsMagR, but not in bacterial eclscA, based on the EPR (Figure 4D–G) and CD spectra (Figure 4B).

EPR spectroscopy can also detect mononuclear iron binding in proteins, with a characteristic peak at $g=4.3$, typically due to mononuclear high-spin ($S=5/2$) Fe^{3+} ions in sites of low symmetry (Bou-Abdallah & Chasteen, 2008; Castner et al., 1960; Drovosekov et al., 2023; Zhou et al., 2023). As shown in Figure 4C, the MagRs of all four representative species exhibited ferric iron binding.

In conclusion, all three types of MagRs from different species showed mononuclear iron binding, but only types 2 and 3 exhibited iron-sulfur cluster binding capacity. The late acquisition of iron-sulfur cluster binding in MagRs seems to have occurred only in eukaryotes during evolution.

MagR stability increases during evolution

Cofactors such as iron-sulfur clusters are crucial for the stability and biological function of proteins. Studying the binding affinity and stability of these cofactors can provide insights into the stability of native proteins (Bushmarina et al., 2006; Mansouri et al., 2022). UV-Vis spectroscopy was applied to monitor the binding and dissociation of iron-sulfur clusters in the three different types of MagRs.

In brief, freshly purified MagR proteins from bacterial eclscA, worm ceMagR, pigeon clMagR and human hsMagR were incubated at room temperature for 156 h (6.5 days) and

monitored by UV-Vis scanning at regular intervals (Figure 5A–D). The decay (or dissociation) curves of the iron and iron-sulfur clusters were generated by re-plotting the absorption value at 330 nm, 420 nm, and 460 nm for comparison (Figure 5E–G). A decrease in UV-Vis absorption indicates the loss of iron-sulfur clusters in the protein.

As shown in Figure 5, the UV-Vis spectra at different time points illustrated the rate at which iron or iron-sulfur clusters were dissociated from the MagR proteins. At the starting point, ceMagR had the highest absorption peak at 330 nm (Figure 5E), while hsMagR had the highest absorption peaks at 420 and 460 nm (Figure 5F, G), indicating strong iron binding in ceMagR and iron-sulfur binding in ciMagR. As incubation time increased, the three types of MagRs lost their absorption at 330 nm at a similar rate, although type 2 ceMagR decreased slightly faster (Figure 5E). The dissociation rate of iron-sulfur clusters in type 2 ceMagR, as shown by the decay of absorption at 420 nm (Figure 5F) and 460 nm (Figure 5G), was much faster than in type 3 ciMagR and hsMagR, suggesting that type 2 MagRs may have looser binding of iron-sulfur clusters, leading to rapid dissociation.

Taken together, our results strongly suggest that the stability of iron-sulfur clusters in MagRs had gradually increased during evolution, indicating that MagRs have become progressively more stable over time.

DISCUSSION

MagRs are highly evolutionarily conserved from bacteria to humans (Lu et al., 2020). Initially, MagRs were identified as scaffold proteins for iron-sulfur cluster assembly and iron donors for iron-sulfur clusters involved in the synthesis of several tricarboxylic acid cycle-related enzymes (Jensen & Culotta, 2000; Krebs et al., 2001; Pelzer et al., 2000). Later research proposed that these proteins serve as a putative

magnetoreceptor in the biocompass model, in complex with Cry (Qin et al., 2016), with the intermolecular electron transport chain between MagRs and Cry posited to play an essential role in magnetoreception (Qin et al., 2016; Xie, 2022). Mutation or knockout of MagRs in humans and mice results in fatal diseases or even embryonic lethality (Lebigot et al., 2020; Lee et al., 2019; Oishi et al., 2016; Sheng et al., 2023). Furthermore, knockdown of MagR expression *in vivo* abolishes orientation in the armyworm (*Mythimna separata*), validating the vital role of MagRs not only as iron-sulfur cluster assembly proteins but also as potential magnetoreceptors.

In the current study, we integrated evolutionary biology with biochemistry to gain a more complete understanding of how MagRs evolved from the prokaryotic ancestor IscA. This integration may illuminate how animal magnetoreception evolved from iron metabolism and an iron-sulfur protein. Specifically, we sought to answer the questions, “How do animal magnetoreception and navigation work?” and “How did they evolve?” (Harms & Thornton, 2013; Jayaraman et al., 2022).

We collected MagR sequences from 131 species and selected 23 representative MagRs from different species, covering prokaryotes to Mollusca, Arthropoda, Osteichthyes, Reptilia, Aves, and mammals for biochemical studies. Using these 23 purified MagR proteins, we demonstrated that total iron content in MagRs has gradually increased during evolution, suggesting that MagRs may play increasingly important roles as species evolve. All MagRs can be classified into three different types, with distinct UV-Vis absorption profiles. Type 1 MagRs were primarily found in prokaryotes, while type 2 MagRs were found in some of invertebrates, such as hydras, worms, and sea slugs, and type 3 MagRs were present in certain invertebrates, such as octopuses and insects, and in all vertebrates. Biochemical analysis revealed that type 1 MagRs only bind to mononuclear iron, while type 2

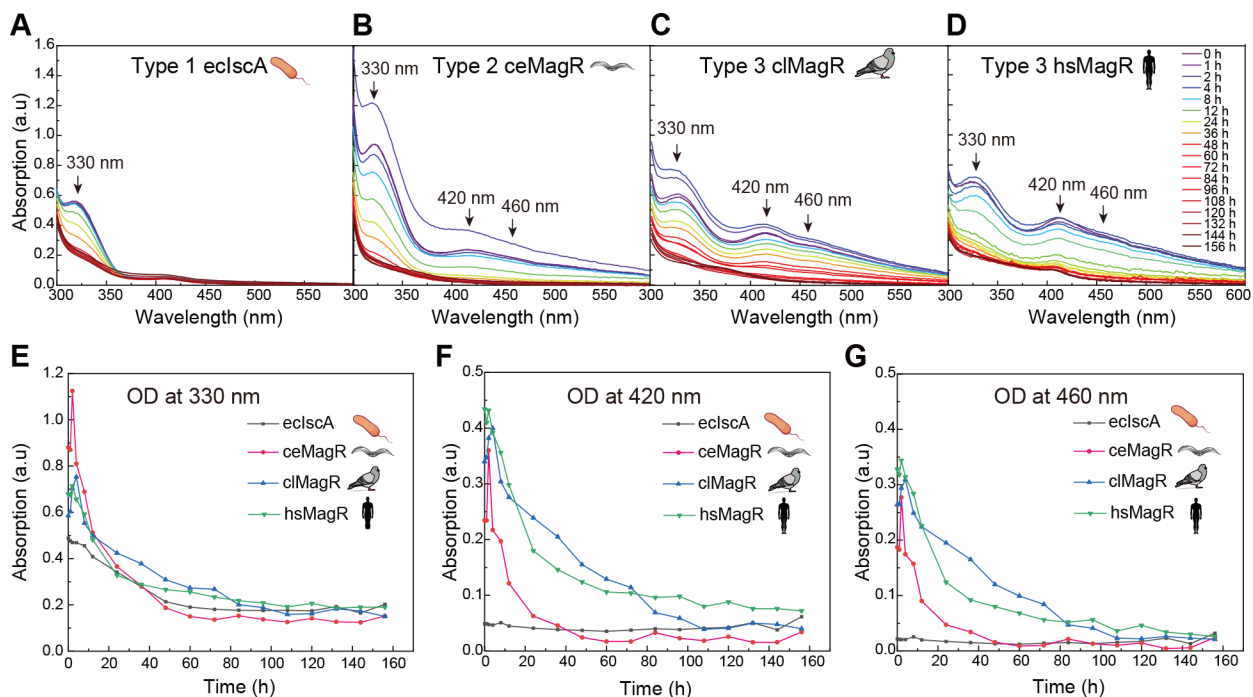


Figure 5 Stability of iron-sulfur binding in three different types of MagRs

A–D: UV-Vis absorption of purified eclscA (A), ceMagR (B), ciMagR (C), and hsMagR (D) recorded at room temperature for 156 h. E–G: Decay curves of UV-Vis absorption of three types of purified MagRs from four species at 330 nm (E), 420 nm (F), and 460 nm (G) during room temperature incubation. Data were derived from (A–D).

MagRs can bind to both iron and iron-sulfur clusters, although iron-sulfur cluster binding is low and unstable. In contrast, type 3 MagRs showed very high iron content, high binding affinity for both mononuclear iron and iron-sulfur clusters, and greater stability. Thus, type 2 MagRs likely represent a transitional form from type 1 in prokaryotes to type 3 in vertebrates. The few exceptions (Figure 2) may suggest selective pressure for magnetoreception and navigation during speciation, warranting further investigation.

Overall, our evolutionary biochemical studies help clarify how evolution has shaped the physiochemical properties of biological molecules such as MagRs and how these properties influence the evolutionary trajectories of MagRs.

SUPPLEMENTARY DATA

Supplementary data to this article can be found online.

COMPETING INTERESTS

The authors declare that they have no competing interests.

AUTHORS' CONTRIBUTIONS

C.X. conceived the idea and designed the study. J.Z., Y.C., and C.H. carried out protein purification and CD spectroscopy. Y.Z., S.W., and M.W. helped with the EPR experiments. T.C., H.M.L., and P.Z. provided valuable suggestions on data analysis. J.Z., T.C., and C.X. wrote the paper. All authors read and approved the final version of the manuscript.

ACKNOWLEDGMENTS

We are grateful to the Steady High Magnetic Field Facilities (High Magnetic Field Laboratory, CAS) for assistance with EPR measurements, as well as Dr. Wei Tong and Jinxing Li for their technical support. We are grateful to the core facilities of the College of Life Sciences at the University of Science and Technology of China, and core facilities of the College of Life Sciences at Anhui University for their help in CD spectral measurements.

REFERENCES

- Alerstam T, Bäckman J, Grönroos J, et al. 2019. Hypotheses and tracking results about the longest migration: The case of the arctic tern. *Ecology and Evolution*, **9**(17): 9511–9531.
- Baker RR. 1980. Goal orientation by blindfolded humans after long-distance displacement: possible involvement of a magnetic sense. *Science*, **210**(4469): 555–557.
- Baker RR. 1988. Human magnetoreception for navigation. *Progress in Clinical and Biological Research*, **257**: 63–80.
- Begall S, Malkemper EP, Červený J, et al. 2013. Magnetic alignment in mammals and other animals. *Mammalian Biology*, **78**(1): 10–20.
- Biro D. 2010. Bird navigation: a clear view of magnetoreception. *Current Biology*, **20**(14): R595–R596.
- Bou-Abdallah F, Chasteen ND. 2008. Spin concentration measurements of high-spin ($g' = 4.3$) rhombic iron(III) ions in biological samples: theory and application. *JBIC Journal of Biological Inorganic Chemistry*, **13**(1): 15–24.
- Brower LP. 1996. Monarch butterfly orientation: missing pieces of a magnificent puzzle. *Journal of Experimental Biology*, **199**(Pt 1): 93–103.
- Burda H, Begall S, Hart V, et al. 2020. Magnetoreception in mammals. In: Fritzsche B. The Senses: A Comprehensive Reference. 2nd ed. Amsterdam: Elsevier, 421–444.
- Burda H, Marhold S, Westenberger T, et al. 1990. Magnetic compass orientation in the subterranean rodent *Cryptomys hottentotus* (Bathyergidae). *Experientia*, **46**(5): 528–530.
- Bushmarina NA, Blanchet CE, Vernier G, et al. 2006. Cofactor effects on the protein folding reaction: acceleration of α -lactalbumin refolding by metal ions. *Protein Science*, **15**(4): 659–671.
- Cadiou H, McNaughton PA. 2010. Avian magnetite-based magnetoreception: a physiologist's perspective. *Journal of the Royal Society Interface*, **7** S2(S2): S193–S205.
- Castner T Jr, Newell GS, Holton WC, et al. 1960. Note on the paramagnetic resonance of iron in glass. *The Journal of Chemical Physics*, **32**(3): 668–673.
- Chae KS, Kim SC, Kwon HJ, et al. 2022. Human magnetic sense is mediated by a light and magnetic field resonance-dependent mechanism. *Scientific Reports*, **12**(1): 8997.
- Cupp-Vickery JR, Silberg JJ, Ta DT, et al. 2004. Crystal structure of IscA, an iron-sulfur cluster assembly protein from *Escherichia coli*. *Journal of Molecular Biology*, **338**(1): 127–137.
- Ding HE, Clark RJ. 2004. Characterization of iron binding in IscA, an ancient iron-sulphur cluster assembly protein. *Biochemical Journal*, **379**(Pt 2): 433–440.
- Ding HE, Yang JJ, Coleman LC, et al. 2007. Distinct iron binding property of two putative iron donors for the iron-sulfur cluster assembly: IscA and the bacterial frataxin ortholog CyaY under physiological and oxidative stress conditions. *Journal of Biological Chemistry*, **282**(11): 7997–8004.
- Drovosekov AB, Kreines NM, Ziganurov DA, et al. 2023. Specific features of $g \approx 4.3$ EPR line behavior in magnetic nanogranular composites. *Journal of Experimental and Theoretical Physics*, **137**(4): 562–571.
- Egevang C, Stenhouse IJ, Phillips RA, et al. 2010. Tracking of Arctic terns *Sterna paradisaea* reveals longest animal migration. *Proceedings of the National Academy of Sciences of the United States of America*, **107**(5): 2078–2081.
- Felsenstein J. 1985. Confidence limits on phylogenies: an approach using the bootstrap. *Evolution*, **39**(4): 783–791.
- Foley LE, Gegeer RJ, Reppert SM. 2011. Human cryptochrome exhibits light-dependent magnetosensitivity. *Nature Communications*, **2**: 356.
- Friis I, Sjulstok E, Solov'yov IA. 2017. Computational reconstruction reveals a candidate magnetic biocompass to be likely irrelevant for magnetoreception. *Scientific Reports*, **7**(1): 13908.
- Guo Z, Xu S, Chen X, et al. 2021. Modulation of MagR magnetic properties via iron-sulfur cluster binding. *Scientific Reports*, **11**(1): 23941.
- Harms MJ, Thornton JW. 2013. Evolutionary biochemistry: revealing the historical and physical causes of protein properties. *Nature Reviews Genetics*, **14**(8): 559–571.
- Hoppe A, Pandelia ME, Gärtner W, et al. 2011. [Fe₄S₄]- and [Fe₃S₄]-cluster formation in synthetic peptides. *Biochimica et Biophysica Acta*, **1807**(11): 1414–1422.
- Hore PJ, Mouritsen H. 2016. The radical-pair mechanism of magnetoreception. *Annual Review of Biophysics*, **45**: 299–344.
- Im J, Lee J, Löffler FE. 2013. Interference of ferric ions with ferrous iron quantification using the ferrozine assay. *Journal of Microbiological Methods*, **95**(3): 366–367.
- Jacklyn PM, Munro U. 2002. Evidence for the use of magnetic cues in mound construction by the termite *Amitermes meridionalis* (Isoptera: Termitinae). *Australian Journal of Zoology*, **50**(4): 357–368.
- Jayaraman V, Toledo-Patino S, Noda-García L, et al. 2022. Mechanisms of protein evolution. *Protein Science*, **31**(7): e4362.
- Jensen LT, Culotta VC. 2000. Role of *Saccharomyces cerevisiae* ISA1 and ISA2 in iron homeostasis. *Molecular and Cellular Biology*, **20**(11): 3918–3927.
- Johnsen S, Lohmann KJ. 2008. Magnetoreception in animals. *Physics Today*, **61**(3): 29–35.
- Kaur G, Iyer LM, Subramanian S, et al. 2018. Evolutionary convergence and divergence in archaeal chromosomal proteins and Chromo-like domains from bacteria and eukaryotes. *Scientific Reports*, **8**(1): 6196.
- Kimchi T, Etienne AS, Terkel J. 2004. A subterranean mammal uses the magnetic compass for path integration. *Proceedings of the National Academy of Sciences of the United States of America*, **101**(4): 1105–1109.

- Kirschvink JL, Gould JL. 1981. Biogenic magnetite as a basis for magnetic field detection in animals. *Biosystems*, **13**(3): 181–201.
- Kirschvink JL, Walker MM, Diebel CE. 2001. Magnetite-based magnetoreception. *Current Opinion in Neurobiology*, **11**(4): 462–467.
- Krebs C, Agar JN, Smith AD, et al. 2001. IscA, an alternate scaffold for Fe-S cluster biosynthesis. *Biochemistry*, **40**(46): 14069–14080.
- Landry AP, Cheng ZS, Ding HE. 2013. Iron binding activity is essential for the function of IscA in iron-sulphur cluster biogenesis. *Dalton Transactions*, **42**(9): 3100–3106.
- Lebigot E, Hully M, Amazit L, et al. 2020. Expanding the phenotype of mitochondrial disease: Novel pathogenic variant in *ISCA1* leading to instability of the iron-sulfur cluster in the protein. *Mitochondrion*, **52**: 75–82.
- Lee J, Ma JS, Lee K. 2019. Direct delivery of adenoviral CRISPR/Cas9 vector into the blastoderm for generation of targeted gene knockout in quail. *Proceedings of the National Academy of Sciences of the United States of America*, **116**(27): 13288–13292.
- Lohmann KJ. 2016. Protein complexes: A candidate magnetoreceptor. *Nature Materials*, **15**(2): 136–138.
- Lohmann KJ, Willows AOD. 1987. Lunar-modulated geomagnetic orientation by a marine mollusk. *Science*, **235**(4786): 331–334.
- Lu HM, Li JD, Zhang YD, et al. 2020. The evolution history of Fe-S cluster A-type assembly protein reveals multiple gene duplication events and essential protein motifs. *Genome Biology and Evolution*, **12**(3): 160–173.
- Lu JX, Bitoun JP, Tan GQ, et al. 2010. Iron-binding activity of human iron-sulfur cluster assembly protein hIscA1. *Biochemical Journal*, **428**(1): 125–131.
- Maeda K, Henbest KB, Cintolesi F, et al. 2008. Chemical compass model of avian magnetoreception. *Nature*, **453**(7193): 387–390.
- Mansouri HR, Carmona OG, Jodlbauer J, et al. 2022. Mutations increasing cofactor affinity, improve stability and activity of a baeyer-villiger monooxygenase. *ACS Catalysis*, **12**(19): 11761–11766.
- Mouritsen H. 2018. Long-distance navigation and magnetoreception in migratory animals. *Nature*, **558**(7708): 50–59.
- Mouritsen H, Ritz T. 2005. Magnetoreception and its use in bird navigation. *Current Opinion in Neurobiology*, **15**(4): 406–414.
- Naisbett-Jones LC, Lohmann KJ. 2022. Magnetoreception and magnetic navigation in fishes: a half century of discovery. *Journal of Comparative Physiology A*, **208**(1): 19–40.
- Nasta V, Da Vela S, Gourdoups S, et al. 2019. Structural properties of [2Fe-2S] ISCA2-IBA57: a complex of the mitochondrial iron-sulfur cluster assembly machinery. *Scientific Reports*, **9**(1): 18986.
- Oishi I, Yoshii K, Miyahara D, et al. 2016. Targeted mutagenesis in chicken using CRISPR/Cas9 system. *Scientific Reports*, **6**: 23980.
- Ollagnier-De-Choudens S, Mattioli T, Takahashi Y, et al. 2001. Iron-sulfur cluster assembly: characterization of IscA and evidence for a specific and functional complex with ferredoxin. *Journal of Biological Chemistry*, **276**(25): 22604–22607.
- Pandelia ME, Nitschke W, Infossi P, et al. 2011. Characterization of a unique [FeS] cluster in the electron transfer chain of the oxygen tolerant [NiFe] hydrogenase from *Aquifex aeolicus*. *Proceedings of the National Academy of Sciences of the United States of America*, **108**(15): 6097–6102.
- Pelzer W, Mühlenhoff U, Diekert K, et al. 2000. Mitochondrial IscA2 plays a crucial role in the maturation of cellular iron-sulfur proteins. *FEBS Letters*, **476**(3): 134–139.
- Qin SY, Yin H, Yang CL, et al. 2016. A magnetic protein biocompass. *Nature Materials*, **15**(2): 217–226.
- Ritz T, Adem S, Schulten K. 2000. A model for photoreceptor-based magnetoreception in birds. *Biophysical Journal*, **78**(2): 707–718.
- Rodgers CT, Hore PJ. 2009. Chemical magnetoreception in birds: the radical pair mechanism. *Proceedings of the National Academy of Sciences of the United States of America*, **106**(2): 353–360.
- Rothery RA, Blasco F, Weiner JH. 2001. Electron transfer from heme b_L to the [3Fe-4S] cluster of *Escherichia coli* nitrate reductase A (NarGHI). *Biochemistry*, **40**(17): 5260–5268.
- Saitou N, Nei M. 1987. The neighbor-joining method: a new method for reconstructing phylogenetic trees. *Molecular Biology and Evolution*, **4**(4): 406–425.
- Schulten K, Weller A. 1978. Exploring fast electron transfer processes by magnetic fields. *Biophysical Journal*, **24**(1): 295–305.
- Sheng HX, Lu D, Qi XL, et al. 2023. A neuron-specific *Isca1* knockout rat developments multiple mitochondrial dysfunction syndromes. *Animal Models and Experimental Medicine*, **6**(2): 155–167.
- Song DS, Tu Z, Lee FS. 2009. Human ISCA1 interacts with IOP1/NARFL and functions in both cytosolic and mitochondrial iron-sulfur protein biogenesis. *Journal of Biological Chemistry*, **284**(51): 35297–35307.
- Walcott C, Gould JL, Kirschvink JL. 1979. Pigeons have magnets. *Science*, **205**(4410): 1027–1029.
- Wang CX, Hilburn IA, Wu DA, et al. 2019. Transduction of the geomagnetic field as evidenced from alpha-band activity in the human brain. *eNeuro*, **6**(2): e0483–18.2019.
- Wang M, Nie YG, Swaisgood RR, et al. 2023. Stable seasonal migration patterns in giant pandas. *Zoological Research*, **44**(2): 341–348.
- Wang S, Zhang P, Fei F, et al. 2024. Unexpected divergence in magnetoreceptor MagR from robin and pigeon linked to two sequence variations. *Zoological Research*, **45**(1): 69–78.
- Weiler BD, Bruck MC, Kothe I, et al. 2020. Mitochondrial [4Fe-4S] protein assembly involves reductive [2Fe-2S] cluster fusion on ISCA1-ISCA2 by electron flow from ferredoxin FDX2. *Proceedings of the National Academy of Sciences of the United States of America*, **117**(34): 20555–20565.
- Westby GWM, Partridge KJ. 1986. Human homing: still no evidence despite geomagnetic controls. *Journal of Experimental Biology*, **120**(1): 325–331.
- Wiltschko R, Wiltschko W. 1995. *Magnetic Orientation in Animals*. New York: Springer.
- Wiltschko W, Wiltschko R. 2005. Magnetic orientation and magnetoreception in birds and other animals. *Journal of Comparative Physiology A*, **191**(8): 675–693.
- Wiltschko R, Wiltschko W. 2006. Magnetoreception. *BioEssays*, **28**(2): 157–168.
- Wiltschko R, Wiltschko W. 2019. Magnetoreception in birds. *Journal of the Royal Society Interface*, **16**(158): 20190295.
- Xie C. 2022. Searching for unity in diversity of animal magnetoreception: from biology to quantum mechanics and back. *The Innovation*, **3**(3): 100229.
- Xu JJ, Jarocha LE, Zollitsch T, et al. 2021. Magnetic sensitivity of cryptochrome 4 from a migratory songbird. *Nature*, **594**(7864): 535–540.
- Zhang YQ, Zhang P, Wang JJ, et al. 2024. Mitochondrial targeting sequence of magnetoreceptor MagR: more than just targeting. *Zoological Research*, **45**(3): 468–477.
- Zhou YJ, Tong TY, Wei MK, et al. 2023. Towards magnetism in pigeon MagR: Iron- and iron-sulfur binding work indispensably and synergistically. *Zoological Research*, **44**(1): 142–152.